# Singular Structure and Enhanced Friedel Oscillations in the Two-Dimensional Electron Gas

I. G. Khalil*, N. W. Ashcroft†, and M. Teter†
*Gene Network Sciences, 2359 N Triphammer Rd, Ithaca, NY 14850
†Cornell Center for Materials Research, and the Laboratory of Atomic and Solid State Physics, Cornell University, Ithaca, NY 14853-2501
(February 1, 2008)

We calculate the leading order corrections (in $r_s$) to the static polarization $\Pi^*(q,0,)$, with dynamically screened interactions, for the two-dimensional electron gas. The corresponding diagrams all exhibit singular logarithmic behavior in their derivatives at $q = 2k_F$ and provide significant enhancement to the proper polarization particularly at low densities. At a density of $r_s = 3$, the contribution from the leading order *fluctuational* diagrams exceeds both the zeroth order (Lindhard) response and the self-energy and exchange contributions. We comment on the importance of these diagrams in two-dimensions and make comparisons to an equivalent three-dimensional electron gas; we also consider the impact these finding have on $\Pi^*(q,0)$ computed to all orders in perturbation theory.

Two-dimensional electron systems with standard singular Coulombic interactions have attracted a great deal of attention in recent years. Of particular interest have been the driving mechanisms behind the high temperature superconductors, the metal-insulator transition exhibited by the two-dimensional localized electrons in semiconductors, and the novel charge and spin-density-wave ordering found in layered compounds. An important question is the degree to which we might attribute this novel behavior specifically to the two-dimensionality and the singular character of the Coulomb interaction? In this letter, we attempt to provide an answer by computing the leading order corrections to the proper static polarization $\Pi^*$ beyond the random-phase approximation (RPA) through inclusion of the diagrams presented in Fig. 1 shown there as the self-energy, exchange, and

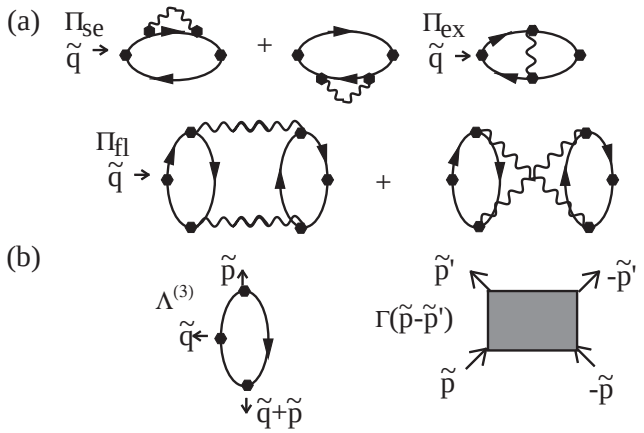


FIG. 1. (a) Leading order corrections to the proper polarization $\Pi^*$. The interaction lines represent RPA screened Coulomb interactions. (b) The three-point diagram $\Lambda^{(3)}$and the effective scattering vertex $\Gamma(q)$ .

fluctuation diagrams, respectively. For the three-dimensional electron gas, these diagrams have been well studied, and in particular have been computed and analyzed in detail (see [1]- [3] and references therein). For a strictly two-dimensional electron gas with $2\pi e^2/q$ interaction, we report here that the response function beyond the RPA exhibits singular structure that is far more pronounced than found from the zeroth order Lindhard response function; these leading order corrections play an important role even at high-densities.

It is not surprising that all three leading order diagrams exhibit similar singular structure since they can be reduced to expressions containing the three-point diagram shown $\Lambda^{(3)}$in Fig. 1 (multiplied by Coulombic interaction lines). This singular structure should extend to all orders in perturbation theory since all higher order corrections to the polarization also reduce to a sum of three-point diagrams $\Lambda^{(3)}$(again multiplied by Coulombic interaction lines). More importantly, the enhancement of the polarization from all of three of the leading order diagrams is already significant at high densities, but as the density is reduced the contribution from the fluctuation diagrams rapidly exceeds that of the self-energy and exchange contributions. This is in marked contrast to the three-dimensional electron gas where fluctuational diagrams provide a small enhancement to the corresponding zeroth order Lindhard response when compared to contributions solely from the exchange and self-energy diagrams (for densities in the metallic range [3]). The increased role that fluctuations are expected to play in two dimensions is evident.

Begin with the static zeroth-order Lindhard response function $\Pi^0$, appropriate to the random-phase approximation. The well-known singular behavior of

$\Pi^0$ leads to possible instabilities arising from electron-electron interactions. In three dimensions, this singularity also leads to a modulation in the long range effective electron-electron interaction which in three dimensions takes the form $V(r) \sim cos(2k_F r)/r^3$. Based on this Kohn and Luttinger [4] were the first to consider the possibility of ground-state electron pairing in the presence of purely repulsive forces where they found attractions in the effective vertex $\Gamma(q)$ of Fig. 1 for large angular momentum quantum numbers. Details of the shape of the Fermi surface (for example, nesting) might well enhance such possibilities.

In two dimensions, and at the level of the Lindhard response function, these effects are not especially prominent. The function $\Pi^0(q)$ is then a constant for $q \leq 2k_F$, and exhibits a square root singularity in the derivative for momentum $q > 2k_F$ [5]. Because of this arguments for possible charge/spin instabilities based on $\Pi^0$ are not compelling. While this square root singularity does lead to a long range component in the effective interaction ($V(r) \sim sin(2k_F r)/r^2$) for two dimensions, the effective interaction vertex $\Gamma(q)$ of Fig. 1 computed at this low order remains independent of momentum at the Fermi surface. Only an s-wave repulsive scattering channel opens at this order and higher-order effects must be considered in order to find attractive scattering channels [6]. But beyond the random phase approximation (RPA) the situation is quite different and we report here that the first order corrections to $\Pi^*$ already give singularities (in part logarithmic) in the derivative on both sides of $2k_F$, and this singular structure is further enhanced according to the number of three-point diagrams $\Lambda^{(3)}$and interaction lines appearing in a polarization diagram. As an example, the fluctuation diagrams $\Pi_{fl}$ of Fig. 1 contains two three-point diagrams and two dynamically screened interaction lines, and shows greater singular behavior at the Fermi surface in two-dimensions than the self-energy and exchange diagrams which depend on a single three-point diagram and single dynamically screened interaction line (see Eqs. 1 and 2). Consequently the enhancement near $2k_F$ in $\Pi^*$ from these diagrams leads to a greater attraction in *real space* for the screened interaction $V_q^* = v_q/(1 - v_q\Pi^*)$ when compared with the RPA effective interaction $V_q^{RPA} = v_q/(1 - v_q\Pi^0)$.

As noted in references [3] and [7], the self energy $\Pi_{se}$ , exchange $\Pi_{ex}$ , and fluctuation $\Pi_{fl}$ diagrams depicted in Fig. 1 can all be written in terms of the three-point function; thus

$$\Pi_{se}(\tilde{p}) = Tr_{\tilde{q}} v_{RPA}(\tilde{q}) \times \left[\frac{\partial}{\partial(i\omega_q)} - \frac{\partial}{\partial(i\omega_p)}\right] \times \left[\Lambda^{(3)}(\tilde{p},\tilde{q}) + \Lambda^{(3)}(\tilde{q},\tilde{p})\right], \quad (1)$$

$$\Pi_{ex}(\tilde{p}) = Tr_{\tilde{q}} \frac{v_{RPA}(\tilde{q})}{\mathbf{p}\cdot\mathbf{q}/m} \times \left[\Lambda^{(3)}(\tilde{p},\tilde{q}) + \Lambda^{(3)}(\tilde{q},\tilde{p}) - \Lambda^{(3)}(-\tilde{p},\tilde{q}) - \Lambda^{(3)}(\tilde{q},-\tilde{p})\right], \quad (2)$$

$$\Pi_{fl}(\tilde{p}) = -\frac{1}{2} Tr_{\tilde{q}} v_{RPA}(\tilde{q}) v_{RPA}(\tilde{p}-\tilde{q}) \times \left[\Lambda^{(3)}(\tilde{q},\tilde{p}-\tilde{q}) + \Lambda^{(3)}(\tilde{p}-\tilde{q},\tilde{q})\right]^2. \quad (3)$$

Here $\tilde{p} = (i\omega_p, \mathbf{p})$ is the energy-momentum variable, $v_{RPA}$ is the screened Coulombic interaction in the random phase approximation (using $v_q = 2\pi e^2/q$), and $Tr_{\tilde{q}}$ stands for the two-dimensional trace over all momentum and energy variables, i.e. $\int d\omega_q/(2\pi) \int d^2q/(2\pi)^2$. The requisite three-point function $\Lambda^{(3)}(\tilde{q},\tilde{p})$ , is given by

$$\Lambda^{(3)}(\tilde{q},\tilde{p}) = -2Tr_{\tilde{k}} G_0(\tilde{k}) G_0(\tilde{k}+\tilde{q}) G_0(\tilde{k}+\tilde{q}+\tilde{p}), \quad (4)$$

where exact analytical expressions for two-dimensional forms are given by Neumayr and Metzner [8]. We compute the diagrams of Fig. 1 in imaginary frequency space to circumvent nonintegrable divergences near $2k_F$ and also when integrating through plasmon peaks in the screened interaction $v_{RPA}(\tilde{q})$. To obtain the static polarizability we simply perform the requisite analytic continuation $\Pi(p, i\omega_p) \rightarrow \Pi(p, \omega + i\delta) = \Pi(p, 0 + i\delta)$.

The numerical procedure for computing $\Pi_{se}$ , $\Pi_{ex}$ , and $\Pi_{fl}$ is lengthy but straightforward. The results for a density of $r_s = 2$ (not a particularly high density) are plotted in Fig. 2 and can be summarized as follows: First, $\Pi_{ex}$ exceeds $\Pi^0$ for momenta up to and slightly above $2k_F$, but $\Pi_{se}$ and $\Pi_{ex}$ have opposite signs and their sum largely cancels. However, $\Pi_{fl}$ at this density, already gives a slightly larger contribution than $\Pi_{se}$ and $\Pi_{ex}$ combined. Second, all three diagrams are finite but discontinuous in slope at $2k_F$; their derivatives diverge logarithmically at all densities. We have determined through a numerical fit that the logarithmic structure is of the form $\sqrt{|q-2k_F|}\log|q-2k_F|$ on either side of $q = 2k_F$. Maldague [9] has numerically computed the 2D self-energy and exchange contributions in the absence of screening and found similar logarithmic divergence in the slope for $q > 2k_F$ by invoking an electrostatic analogy that treats the integrals over $(\Pi_{se} + \Pi_{ex})$ as equivalent charge distributions of radius $k_F$ concentrated near the origin times the 2D bare interaction. The divergence in the slope is stronger above $2k_F$ in overall magnitude than below $2k_F$ due to the analytic form of $\Lambda^{(3)}$which contains non-trivial expressions involving square root singularities (similar to that found in $\Pi^0$ ). These expressions contribute to the analytic form of $\Lambda^{(3)}$above, but not below $2k_F$. Overall the divergent structure is greatest for $\Pi_{fl}$ as

stated earlier. The contribution from all three diagrams is significant already at $r_s = 2$. The role of fluctuations

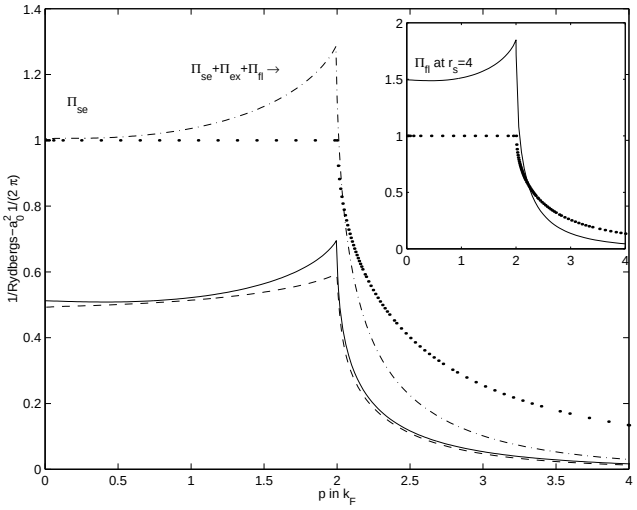


FIG. 2. The solid curve is the static $\Pi_{fl}$ , the dashed curve shows $(\Pi_{se} + \Pi_{ex})$, and the dashed-dotted curve is the sum of all three of the first order correction all at $r_s = 2$. The inset contains the fluctuation diagram at a lower density of $r_s = 4$. The dotted curve is the 2D Lindhard response.

is expected to progressively dominate with decreasing density, and this is apparent at $r_s = 3$ where the fluctuation diagrams begin to exceed $\Pi^0$ . By $r_s = 8$ (a typical density for high-temperature superconductors or the two-dimensional electron(hole) gases in MOSFETS) it is a factor of four greater than $\Pi^0$ where at this density the sum of the self-energy and exchange diagrams only just begins to exceed the zeroth order Lindhard response. Overall the effect of dynamical screening as $r_s$ increases is to reduce the total enhancement of the polarization diagrams as well as the degree of divergence in the slope (see [9] for a comparison with the self-energy and exchange diagrams computed with the bare interaction).

The leading order corrections to the polarization beyond the RPA are not as significant in three-dimensions. In the absence of screening the enhancement $(\Pi_{se} + \Pi_{ex})/\Pi^0$ is $0.17r_s$ at $p = 0$ compared with $0.45r_s$ in 2D , and then proceeds to sharply falls off to half its value at $2k_F$ [2]. The singular structure found in these diagrams resembles that of the 3D Lindhard response, but with dynamical screening the overall enhancement of these diagrams is greatly reduced as shown in Fig. 3 (the data is from reference [3]). This data is representative of the entire metallic density range and confirms the expectation that self-energy and exchange effects are more pronounced in 2D. More striking is the significant enhancement of $\Pi^0$ in 2D from the fluctuation diagrams as seen by comparing the plots of Fig. 2 with the three-dimensional data of Fig. 3. Physically, the diagrams of $\Pi_{fl}$ can be thought of as representing quantum fluctuations in the screening clouds surrounding two interacting electrons, and we expect such effects to play a greater

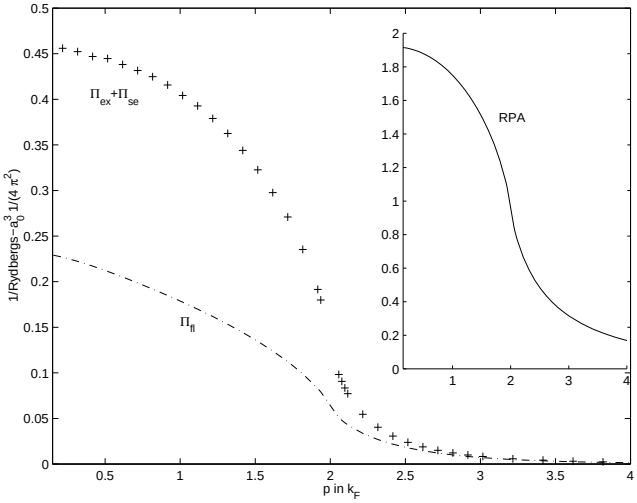


FIG. 3. The Static -$\Pi_{se}$ +$\Pi_{ex}$ , and $\Pi_{fl}$ in 3D at $r_s = 2$. The inset shows the 3D Lindhard response.

role in 2D [10,11]. Enhanced fluctuations in two-dimensions are responsible for the destruction of superconducting phase coherence and long range crystalline order for $T > 0$, and thus it is not surprising to see this theme played out here as well [12,13].

As mentioned earlier, the general structure of these leading order diagrams is an integral over three-point functions $\Lambda^{(3)}$augmented by Coulombic interaction lines. For higher orders, an explicit reduction formula derived by Neumayr and Metzner [8] holds that the general N-loop diagram can be expressed in terms of 3-loop diagrams over an appropriate energy/momentum transfer factor (i.e. in $\Pi_{ex}$ that factor is $(\mathbf{p}\cdot\mathbf{q})$ in Eq.(2)) and thus the structure of all higher order diagrams will be of similar form (for an explicit formula see reference [8]). We therefore expect the singular logarithmic features found in these lower order diagrams to be present in *all* higher order corrections. Cancellations between some of the higher order diagrams may well reduce the overall singular behavior of the total proper polarization $\Pi^*$.

As further higher order corrections are considered there will continue to be significant cancellation between vertex and self-energy diagrams in such a way that their sum makes a smaller net contribution, and any reasonable higher order calculation to $\Pi^*$ should include the right mix of vertex and self-energy diagrams(as is the case for the conserving approximation of Baym and Kadanoff, for example) [14]. But the contribution from diagrams of the fluctuation type differs in two respects. First, the internal Coulomb lines are screened and already represent the sum of an entire class of diagrams in a Dyson series sense [10]; second, higher order contributions of

diagrams from the fluctuational type do not cancel but actually sum to contribute to quantities such as the pair correlation function at zero separation, $g(0)$ [15]. We generally expect, therefore, that contributions from all

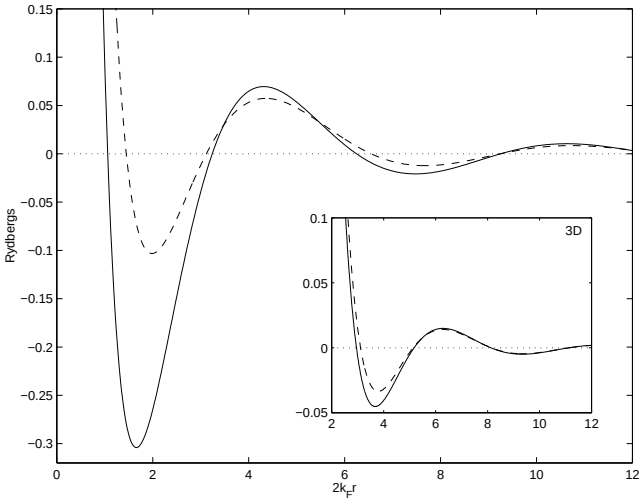


FIG. 4. The screened effective interaction in real space showing an enhancement in the amplitude of the Friedel Oscillations due to the singular structure in $\Pi^*$ at $r_s = 2$ (the dashed line is the RPA screened interaction). The inset shows the three dimensional case at an equivalent density.

such diagrams (e.g. the ladder series) will significantly contribute to the total proper polarization $\Pi^*$ leading to an overall enhancement and to singular logarithmic structure at $2k_F$.

Finally, we return to the important Kohn-Luttinger question for the two dimensional case, but in the context of the leading order corrections of Fig. 1. The effective interaction vertex $\Gamma(q)$ in the case of the electron gas must include a sum of all polarization diagrams due to the singularity at small momentum transfer $\mathbf{q} = \mathbf{p} - \mathbf{p}'$. If we include the leading order contributions to $\Gamma(q)$ we obtain $\Gamma(q) = v_q/(1 - v_q\Pi^*(q))$ with $\Pi^* = \Pi^0 + \Pi_{se} + \Pi_{ex} + \Pi_{fl}$. The logarithmic singularity in $\Pi^*$ now gives rise to a an attraction in $\Gamma_l$ for even angular momentum $l$ starting at $l = 2$ $(d-wave)$, behavior not possible if only $\Pi^0$ entered into the argument. These singularities also significantly contribute to the modulation in real space of the equivalent effective interaction (i.e. $V(q) = v_q/(1 - v_q\Pi^*)$) now plotted in Fig. 4 for $r_s = 2$. The principal depth (the first minimum) of the effective interaction is striking, and the effect is further enhanced as the fluctuation diagrams exceed $\Pi^0$ for densities as low as $r_s = 3$. The inset in Fig. 4 shows the three-dimensional case for comparison where the singularity at $2k_F$ from the leading order corrections leads to only a small enhancement of the Friedel oscillations.

To summarize, the low order diagrams, reducible to similar integral forms, all exhibit singular logarithmic behavior at $2k_F$ and provide significant enhancement over the zeroth order Lindhard response. Real systems either have either a finite transverse extent or exhibit a multi-layered structure. To account for this, we have substituted approximate but more realistic forms for the potential in the diagrams of Fig. 1 more appropriate to 2D electrons in metal-oxide-semiconductors, in thin metallic films, or in layered superlattices. Similar results are found for systems where realistic thicknesses and superlattice spacings are used except that the overall enhancement from these diagrams compared to $\Pi^0$ is reduced depending on the thickness (or spacing between the planes), dielectric constant, and the effective mass of the system. Our results extend to other two-dimensional systems and apply to the 2D electron or hole gas systems found in metal-oxide-semiconductors. The debate over the nature of the metallic state in the recently observed metal-insulator transition of 2D electron or hole semiconductor systems still ensues with explanations ranging from superconductivity to more exotic non-Fermi liquid behavior. The present results may bear on (and lend support to) explanations of the former type. More importantly, we note that accurate data at $2k_F$ is of considerable interest, particularly from Monte Carlo simulations. Large error bars generally accompany polarization data from Monte Carlo simulations in the intermediate regime around $2k_F$ and make difficult an accurate determination of quantities such as local field factor corrections and corresponding effective interactions that could lay to rest debates concerning the likelihood of superconductivity or other electronic instabilities in these systems.

This work is supported by the National Science Foundation under Grant DMR-9988576.

[1] D. C. Langreth, Phys. Rev. Lett. **59**,497 (1987).
[2] E. Engel and S. H. Vosko, Phys. Rev. B **42**, 4940 (1990).
[3] C.F. Richardson and N. W. Ashcroft, Phys. Rev. B **50**, 8170 (1994).
[4] W. Kohn and J. H. Luttinger, Phys. Rev. Lett. **15**, 524 (1965).
[5] F. Stern, Phys. Rev. Lett **18**, 546 (1967).
[6] A. V. Chubukov, Phys. Rev. B. **48**, 1097 (1993).
[7] R. Cenni and P. Saracco, Nucl. Phys. A **487**, 279 (1988); R. Cenni and P. Saracco, Rivista Del Nuovo Cimento **15**,N 12 (1992).
[8] A. Neumayr and W. Metzner, Phys. Rev. B **58**, 15449 (1998).
[9] P. F. Maldague, Solid State Comm. **26**, 133 (1978).
[10] K. Rapcewicz and N.W. Ashcroft, Phys. Rev. B **44**, 4032.
[11] F. Cornu and Ph. A. Martin, Phys. Rev. A **44**, 4893.
[12] P.C. Hohenberg, Phys. Rev. **158**, 383 (1967).
[13] N.D. Mermin, Phys. Rev. **176**, 250 (1968);

[14] G. D. Mahan, Comments Cond. Mat. Phys. **16**,333 (1994).

[15] L. Calmels and A. Gold, Phys. Rev. B **57**, 1436, (1998).